

# DEVELOPMENT OF ULTRA-WIDEBAND SOFTWARE DEFINED RADAR TESTBED TO SUPPORT SAR TOMOGRAPHIC MISSION FORMULATION

Samuel Prager<sup>1</sup>, Brian Hawkins<sup>1</sup>, Matthew Anderson<sup>2</sup>, Soon-Jo Chung<sup>1,2</sup>, and Marco Lavalle<sup>1</sup>

<sup>1</sup>Jet Propulsion Laboratory, California Institute of Technology, Pasadena, CA, USA

<sup>2</sup>California Institute of Technology, Pasadena, CA, USA

## ABSTRACT

Recent innovations in small satellite, ultra-wideband direct RF sampling, and synchronization technologies have made multistatic and MIMO coherent SAR constellations a feasible concept for future missions. The Distributed Aperture Radar Tomographic Sensors (DARTS) mission concept at NASA JPL aims to measure Earth's surface topography and vegetation using TomoSAR techniques. This paper describes the development of an embedded ultra-wideband next generation software defined radar (SDRadar) testbed capable of multi-band operation implemented with the Xilinx RF System on Chip (RFSoC) architecture, which features 8x 6.4 GSPS DACs and 8x 4 GSPS ADCs. The RFSoC SDRadar represents a state of the art testbed for rapid prototyping of radio, radar, and synchronization technologies. We provide preliminary testing results for airborne monostatic radar imaging from a small uninhabited aerial system (sUAS), successfully demonstrating multi-band operation using first and second Nyquist zone direct RF sampling.

**Index Terms**— RFSoC, Software Defined Radar, Synthetic Aperture Radar, SAR, sUAS

## 1. INTRODUCTION

The use of Synthetic aperture radar (SAR) for remote sensing and imaging of the earth in all-weather conditions and through dense foliage has been extensively studied and documented in literature[1]. Properties of earth's forests, including biomass, are important variables in climate science studies and SAR is an essential tool for mapping these properties on a global scale [2]. Recent developments in tomographic SAR (TomoSAR) [3] have extended SAR concepts to the cross-track dimension to enable three-dimensional imaging of forest canopies. New SAR missions, including the ESA BIOMASS satellite mission, will utilize TomoSAR techniques to measure forest biomass globally [4, 5].

The Distributed Aperture Radar Tomographic Sensors (DARTS) mission concept is seeking to extend the monostatic TomoSAR concept to a constellation of coherent

multistatic radar sensor satellites [6]. The use of multi-satellite constellations has the potential to overcome the issue of temporal decorrelation that is inherent to monostatic SAR satellite tomographic imaging due the ability of a multistatic constellation to perform TomoSAR imaging from a single pass rather than multiple passes over several weeks or months [7].

Furthermore, recent advances in digital RF sampling technologies that enable multi-GHz rate sampling have enabled a new class of ultra-wideband software defined radios (SDRs) and software defined radars (SDRadar). The DARTS mission concept has begun to explore the use of ultra-wideband multi-GHz sample rate RF technologies for SDRadar-based TomoSAR imaging. This next-generation SDRadar testbed improves upon a previously reported SDR-based testbed [7] significantly, with a 10× increase in radar pulse repetition frequency (PRF) and an 80× increase in instantaneous bandwidth. We implement this next-generation testbed in a battery-powered embedded system based on the Xilinx RF System on Chip (RFSoC). In this work, we describe the system architecture and provide preliminary results from tests with the RFSoC SDRadar system flown as a payload on a small uninhabited aerial system (sUAS).

## 2. HARDWARE

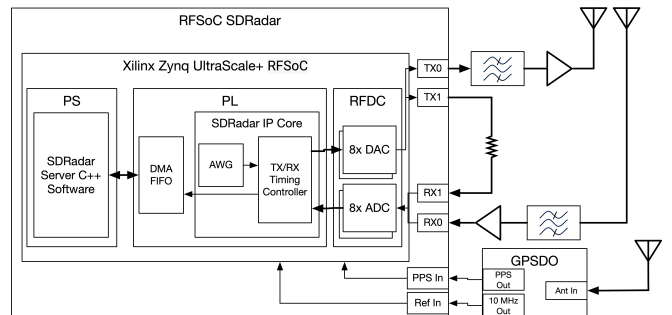


**Fig. 1:** RFSoC-based SDRadar System Diagram.

The hardware basis for the SDRadar system is the Alphatec Data ADM-XRC-9R1 system on module (SoM), which

is based on the Xilinx Zynq UltraScale+ RFSoC chip. The RFSoC features eight 6.4 GSPS RF digital-to-analog converters (DACs) and eight 4 GSPS RF analog-to-digital converters (ADCs) along with a field programmable gate array (FPGA)-based programmable logic (PL) subsystem and a quad-core ARM processing system (PS) integrated onto a single chip.

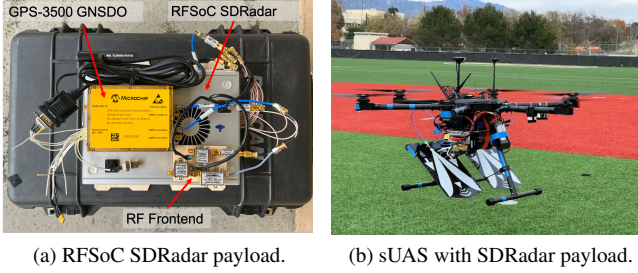


**Fig. 2:** SDRadar payload and sUAS system with integrated radar payload

In our implementation, both the DACs and ADCs are clocked at 4 GHz and operate in complex baseband mode, yielding 2 GHz of usable bandwidth. The RFSoC on-chip RF data converters (RFDCs) also feature numerically controlled oscillator (NCO)-based digital mixers for intermediate frequency (IF) signal conversion from baseband. The RFDC cores are real-time configurable allowing for dynamic multi-band operation and can operate in both even and odd Nyquist zones.

The core component of the SDRadar implementation is the SDRadar IP core implemented in FPGA fabric. This core features a 132k 32-bit complex sample block random access memory (BRAM)-based arbitrary waveform generator (AWG) which is dynamically loadable with arbitrary waveform samples. The SDRadar core controls transmit (TX) and receive (RX) pulse timing and accepts a custom instruction set that configures the pulse repetition interval (PRI), or equivalently the pulse repetition frequency (PRF), number of pulses, and maintains time coherence between the TX and RX channels. Additionally a digital switch IP core controls the data paths between the eight RX and TX channels, enabling loopback calibration as well as multi-antenna or multi-polarization configurations.

The SDRadar FPGA IP Core is controlled by a C++ SDRadar Server application running on the ARM PS. The SDRadar server application both configures the FPGA and RFDC cores of the RFSoC and responds dynamically to requests from clients connected via WiFi, ethernet, or an XBee serial radio link. This includes configuring the waveform, PRI, number of samples, and center frequency as well as initiating radar collection tasks which are stored locally to an on-board SD card. Client-server interaction is similar to that described previously in [8, 9, 10].

An external GPS/GNSS-disciplined oscillator(GPSDO/

GNSSDO) is added to the system to provide GNSS-locked 10 MHz and 1 pulse per second (PPS) references as well as GNSS timing and position data to the SDRadar system. Additionally low noise amplifiers (LNAs) and bandpass filters are added to the TX and RX signal paths. The entire payload is powered using a six cell LiPo 2600 mAh 22.2V battery pack. The RFSoC-based SDRadar testbed system design is shown in Fig. 1. The complete SDRadar system payload is shown in Fig. 2a.

An Aurelia X6 hexacopter from UAV Systems International is used as the sUAS platform. The sUAS system features a Cube Orange flight controller and runs ArduCopter as the flight stack. The sUAS platform has a payload capacity of 5 kg and has a maximum speed of 15 m/s and a 30 minute flight time. The sUAS system is shown in flight with the SDRadar payload in Fig. 2b. We use TSA600 Vivaldi antennas from RFSpace, which have an operating frequency from 600-6000 MHz. The antennas are mounted using a carbon fiber boom system designed by Caltech with additional stabilizing braces to reduce vibration during flight as can be seen in Fig. 2b.

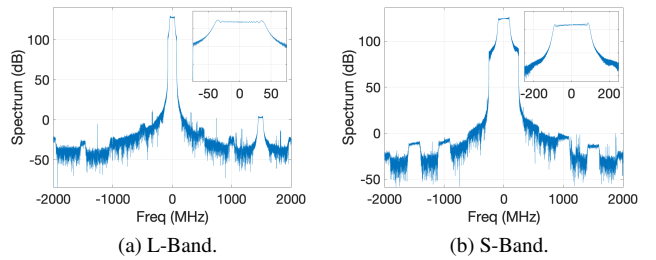


**Fig. 3:** Loopback Spectrum

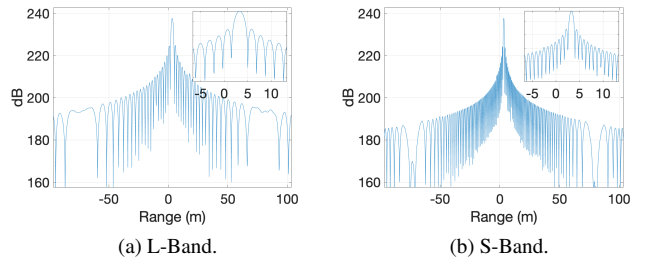


**Fig. 4:** Loopback Matched Filter

### 3. LOOPBACK PERFORMANCE

We characterize the performance of the SDRadar using a loopback calibration channel as shown in Fig. 1. We show the loopback spectrum after low pass filtering for both L-band

(1257.5 MHz center frequency with a 80 MHz bandwidth linear frequency modulated (LFM) chirp, first Nyquist zone) and S-band (3200 MHz center frequency with a 200 MHz bandwidth LFM chirp, second Nyquist zone) in Fig. 3a and Fig. 3b, respectively. The compressed pulse matched filter outputs are shown for L-band and S-band in Fig. 4a and Fig. 4b, respectively.

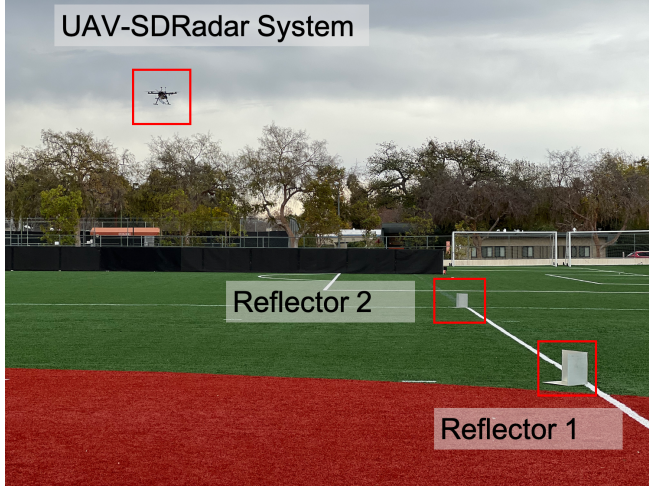


**Fig. 5:** Test scene with UAV-SDRadar system in flight as sUAS payload and two corner reflector targets.

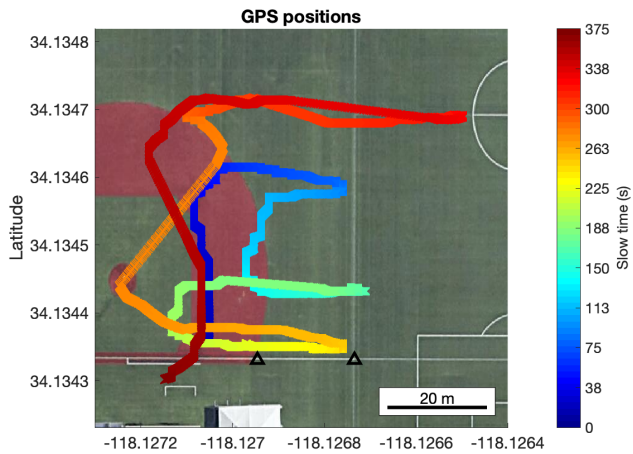


**Fig. 6:** Google Earth overlay of the sUAS path for S-band experimental flight.

#### 4. AIRBORNE MONOSTATIC RADAR EXPERIMENTS

UAV flight experiments using the RFSoC SDRadar payload were carried out at Caltech athletic fields. Two small trihedral corner reflectors were placed on the south field. The sUAS system flew multiple tracks perpendicular to the corner

reflectors at approximately 1.5 m/s and at varying altitudes from 5-30 m for a ~ 6 minute flight. The test scene with both the sUAS UAV-SDRadar system and the corner reflectors is shown in Fig. 5. The GPS positions of the UAV-SDRadar system as measured by the onboard GPSDO, which were stored by the SDRadar for each pulse as metadata, are shown in Fig. 6.

The SDRadar operated at a 133.33 Hz PRF (7.5 ms PRI). We provide results for the S-band configuration, in which case the radar operated in the second Nyquist zone at a center frequency of 3.2 GHz (800 MHz center frequency offset relative to DC) with 3-4.3 GHz bandpass filters used in both the TX and RX paths.

Fig. 7 shows the unfocused radar image collected over multiple passes of the sUAS. The sUAS made 8 total passes across the target scene at varying heights and distances as shown in Fig 6. As highlighted in Fig. 7, the two corner reflectors are clearly seen in the unfocused S-band radar image throughout the flight. Preliminary analysis of the unfocused radar data has demonstrated phase coherence of the target responses indicating the suitability of the retrieved radar data for SAR and interferometric processing.

#### 5. CONCLUSION

The DARTS project has demonstrated an embedded 4 GHz bandwidth capable SDRadar testbed that is suitable as a payload on a sUAS platform. We have demonstrated preliminary monostatic radar imaging with this payload from an aerial platform demonstrating that it can be used successfully in second Nyquist zone operation for radar imaging. The results are encouraging, with preliminary analysis indicating suitability for advanced coherent radar processing including SAR, TomoSAR, and interferometric radar modes. Future work includes demonstration and characterization of SAR performance metrics and interferometric processing with the system as well as integration of previously reported synchronization techniques and multistatic/MIMO radar demonstrations. Additionally, we intend to implement an on-chip multi-band GNSS receiver.

#### 6. REFERENCES

- [1] I. Woodhouse, *Introduction to Microwave Remote Sensing*, Chapman and Hall/CRC, Boca Raton, 2017.
- [2] H. H. Shugart, S. Saatchi, and F. G. Hall, “Importance of structure and its measurement in quantifying function of forest ecosystems,” *Journal of Geophysical Research: Biogeosciences*, vol. 115, no. G2, June 2010.
- [3] A. Reigber and A. Moreira, “First demonstration of airborne SAR tomography using multibaseline L-band data,” *IEEE Transactions on Geoscience and Remote Sensing*, vol. 38, no. 5, pp. 2142–2152, 2000.

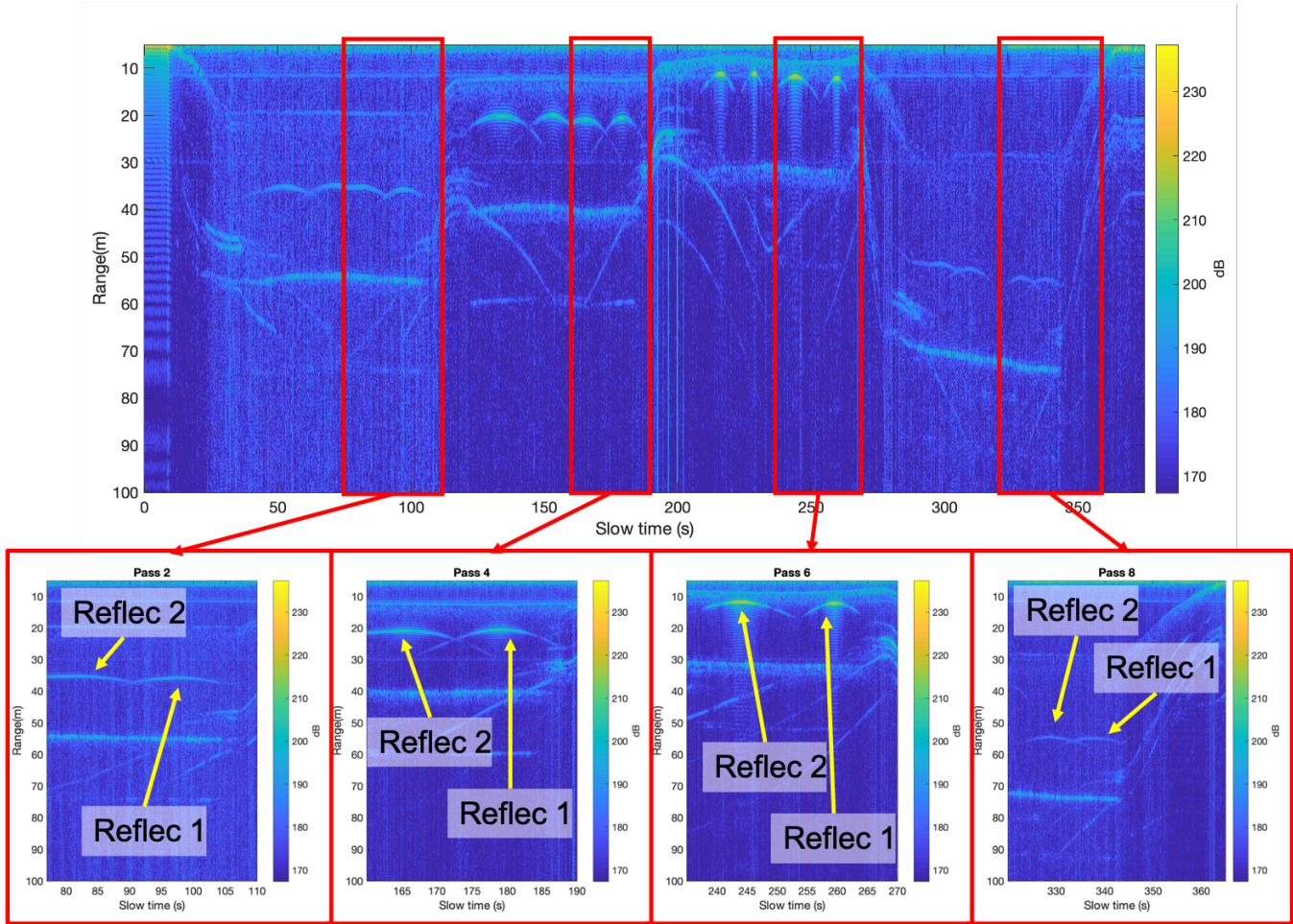


**Fig. 7:** Monostatic S-band radar image collected from eight passes during the sUAS flight.

- [4] K. Scipal, M. Arcioni, J. Chave, J. Dall, F. Fois, T. LeToan, C. Lin, K. Papathanassiou, S. Quegan, F. Rocca, S. Saatchi, H. Shugart, L. Ulander, and M. Williams, “The BIOMASS mission — an ESA Earth Explorer candidate to measure the BIOMASS of the earth’s forests,” in *2010 IEEE International Geoscience and Remote Sensing Symposium*, 2010, pp. 52–55.
- [5] D. Ho Tong Minh, S. Tebaldini, F. Rocca, T. Le Toan, L. Vilillard, and P. C. Dubois-Fernandez, “Capabilities of biomass tomography for investigating tropical forests,” *IEEE Transactions on Geoscience and Remote Sensing*, vol. 53, no. 2, pp. 965–975, 2015.
- [6] Marco Lavalle, Ilgin Seker, James Ragan, Eric Loria, Razi Ahmed, Brian P. Hawkins, Samuel Prager, Duane Clark, Robert Beauchamp, Mark Haynes, Paolo Focardi, Nacer Chatat, Matthew Anderson, Kai Matsuka, Vincenzo Capuano, and Soon-Jo Chung, “Distributed aperture radar tomographic sensors (darts) to map surface topography and vegetation structure,” in *2021 IEEE International Geoscience and Remote Sensing Symposium IGARSS*, 2021, pp. 1090–1093.
- [7] Brian Hawkins, Matthew Anderson, Sam Prager, Soon-Io Chung, and Marco Lavalle, “Experiments with small uas to support sar tomographic mission formulation,” in *2021 IEEE International Geoscience and Remote Sensing Symposium IGARSS*, 2021, pp. 643–646.
- [8] Samuel M Prager, *Ultra-Wideband Multistatic and MIMO Software Defined Radar Sensor Networks*, Ph.D. thesis, University of Southern California, Los Angeles, California, Oct. 2021.
- [9] Samuel Prager, Tushar Thrivikraman, Mark S. Haynes, John Stang, David Hawkins, and Mahta Moghaddam, “Ultrawideband Synthesis for High-Range-Resolution Software-Defined Radar,” *IEEE Transactions on Instrumentation and Measurement*, vol. 69, no. 6, pp. 3789–3803, June 2020.
- [10] Samuel Prager, Graham Sexstone, Daniel McGrath, John Fulton, and Mahta Moghaddam, “Snow depth retrieval with an autonomous uav-mounted software-defined radar,” *IEEE Transactions on Geoscience and Remote Sensing*, pp. 1–16, 2021.